TÜBİTAK

Turkish Journal of Earth Sciences

http://journals.tubitak.gov.tr/earth/

Research Article

Turkish J Earth Sci
(2021) 30: 204-214

doi:10.3906/yer-2006-7

Time frame for future large earthquakes near İstanbul based on east-to-west decelerating failure of the North Anatolian Fault

Fatih BULUT*, Aslı DOĞRU
Geodesy Department, Kandilli Observatory and Earthquake Research Institute, Boğazici University, İstanbul, Turkey

Received: 10.06.2020 • **Accepted/Published Online:** 06.11.2020 • **Final Version:** 22.03.2021

Abstract: Large earthquakes that have occurred along the North Anatolian Fault (NAF) were analysed to elaborate the time frame of future large earthquakes near İstanbul. The historical earthquake catalog that was compiled covered 1 nearly complete and 2 fully complete failures of the NAF between 1250 and 2000 AD. These data were used to investigate the space-time systematics of M ≥ 7.0 earthquakes. The catalogue identified an east-to-west decelerating domino-like failure of the NAF. The deceleration starts around the western tip of the 1944 Gerede rupture. This suggested that failure of the remaining unruptured ~250-km section in the west (İstanbul to Saros) will take substantially longer than failure of the already ruptured ~950-km section in the east (Karlıova to İzmit). The calculations indicated that complete failure of the NAF will last for 243 ± 3 years. The deceleration could not be explained by strain partitioning between the subparallel strands of the NAF in the Marmara region.

Key words: Future earthquakes near İstanbul, North Anatolian Fault, historical earthquakes

1. Introduction

The forecasting of future large earthquakes is significantly relevant for human life in seismically active regions. Although previous efforts have mostly failed due to irregularity in the Earth's dynamics, earthquake forecasting is still a fundamental target of earthquake scientists (e.g., Jackson, 2003). In this study, large earthquakes over the last millennium were quantitatively analysed to quantify a time frame for future large earthquakes along the North Anatolian Fault (NAF), which is a ~1200-km long plate boundary generating devastating earthquakes in northern Turkey (Figure 1).

The magnitude of past earthquakes can be used to determine the present-day slip deficit for defined fault dimensions and therefore, to forecast the slip, as well as the magnitude, of expected earthquakes. Earthquake magnitude is basically a function of the ruptured fault size and slip (Aki, 1966). As the total size of a transform fault is constant, earthquake magnitudes can be used to obtain the cumulative seismic slip, to see whether it matches with the geodetic slip. The historical earthquake catalog that was compiled herein included all M ≥7 earthquakes along the NAF that occurred between 1250 and 2000 AD. Moreover, the NAF failed as an east-to-west migrating series of large earthquakes (Toksöz et al., 1979; Stein et al., 1997; Barka et al., 2002). This pattern was observed during last 2 complete, and partly during the current, incomplete failures, and suggested a stochastic relation between the location and occurrence times of large earthquakes.

In this study, the residual between the seismic and geodetic slip was used to determine the magnitudes of potential earthquakes. In a second step, the time and space characteristics of this stochastic pattern were analysed to elaborate the time frame for the remaining earthquakes on the NAF to complete the current failure.

2. Present-day slip deficit

Moment magnitudes of large earthquakes were used to determine the cumulative seismic slip along the NAF since 1250 AD (Table 1, Figure 2a). All available information in the literature was compiled for M ≥7.0 earthquakes along the NAF, comprising the research of Gutzwiller (1921), Barka (1996), Ambraseys and Jackson (1998), Kondorskaya and Ulomov (1999), Akyuz et al. (2002), Barka et al. (2002), Grünthal and Wahlström (2012), Yaltırak (2015), and Bulut et al. (2019). The 1894 M 7.1 earthquake ruptured the northern boundary of the Çınarcık Basin, according to the intensity map by the Kandilli and Athens observatories. This segment is a normal fault and does not accommodate a dextral motion (e.g., Barka, 1992; Parke et al., 1999). Since the investigation herein was of dextral

* Correspondence: bulutf@boun.edu.tr

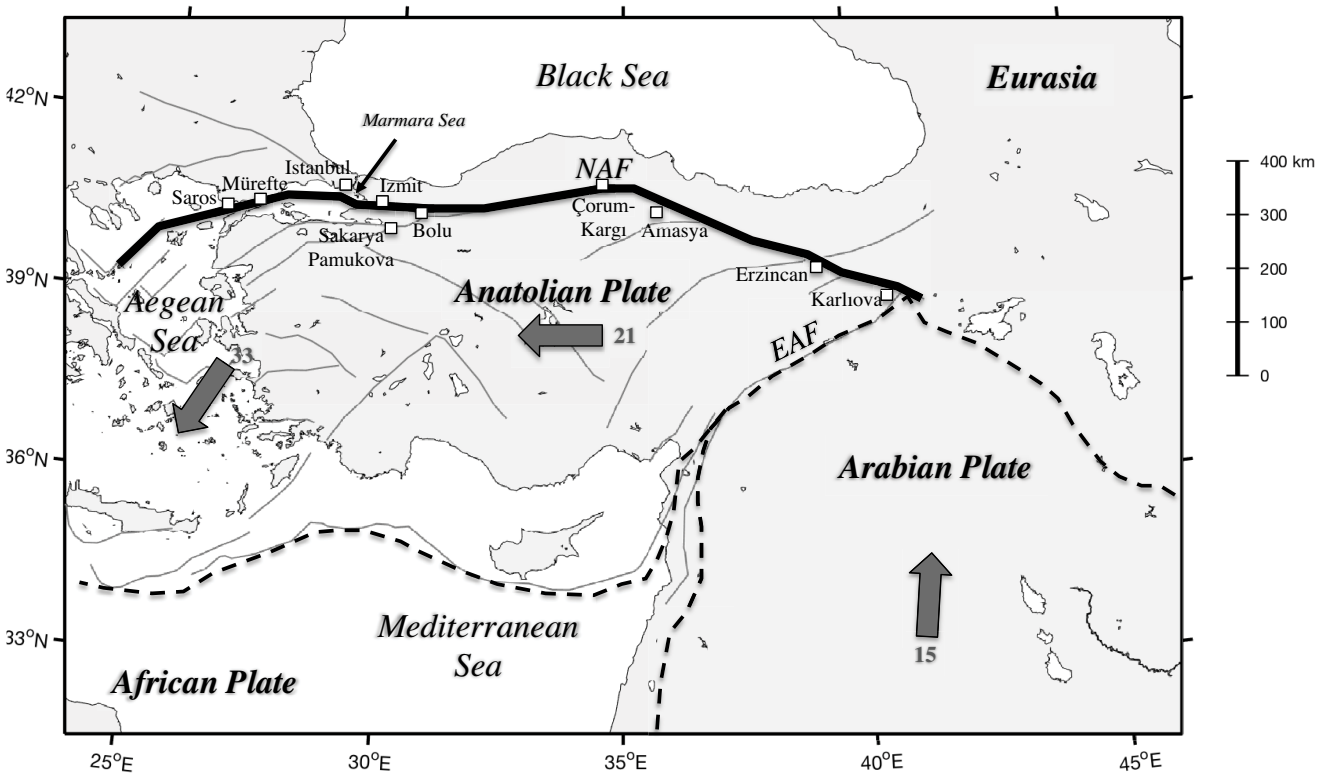

Figure 1. Tectonic sketch of the Anatolian region compiled from work of Reilinger et al., (2006), Bulut et al. (2012), and Yaltırak et al. (2012). Gray lines show major active faults and the black line shows the North Anatolian Fault (NAF) (EAF: East Anatolian Fault). Dashed lines represent plate boundaries, except for the NAF, a boundary between Eurasia and Anatolian Plates, which is indicated by the thick black line. Gray arrows and corresponding numbers indicate GPS-derived plate motions and their horizontal velocities (mm/year) with respect to stable Eurasia.

motions, the extensional 1894 earthquake was therefore excluded in this analysis (Yaltırak and Sahin, 2017).

According to geological and seismological studies that have been conducted, the NAF is a 1200-km-long transform fault zone coupled with a 10-km average depth range (Ketin, 1948; Şengör, 1979; Taymaz et al., 1991; Barka 1992; Aktar et al., 2004; Bulut et al., 2007; Bulut et al; 2018).

Seismic moments of historical earthquakes were used to estimate the event-based average slip along the NAF and time history of the cumulative slip. Seismic moments (M_0 in *Nm*) were obtained from the earthquake magnitudes (M_w), as follows (Kanamori, 1983):

$$\log(M_0) = 3/2\ M_w + 16.1 \quad (1)$$

The average slip was calculated for the fault area (A) of 1200 × 10.0 ± 1.0 km, following the calculation of Aki (1966):

$$M_0 = \mu A d \quad (2)$$

Here, the shear modulus (μ) was assumed to be 32 GPa in the Earth's crust. Event-based slips (d) were cumulatively used to investigate the history of seismic slip along the entire NAF over the last millennium (Figure 2b).

The cumulative seismic slip was compared with the expected geodetic slip to determine the present-day slip deficit and therefore, the magnitudes of potential large earthquakes along the unruptured section of the NAF during the present incomplete failure (Figure 2c). Figure 2b shows the analysed earthquakes, corresponding cumulative slip, and their comparison with the geodetic slip along the NAF. The analysis showed that there is currently a 1.3-m average slip deficit between the geodetic slip and the slip that has been released by historical earthquakes along the entire fault, between 1250 and 2000 AD, which can be released by future earthquakes. However, the fault sections along the NAF last failed at different occurrence times and therefore, must have accumulated different slip deficits.

Table 1. Historical earthquake catalogue.

Year	Month	Day	Latitude (°)	Longitude (°)	Magnitude	Reference	Rupture length (km)	Reference
1254	-	-	39.70	39.50	7.5	Barka, 1996	-	-
1254	-	-	40.00	38.30	7.2	Akyüz et al., 2002	-	-
1296	6	1	40.50	30.50	7.1	Grünthal and Wahlström, 2012	-	-
1343	-	-	40.70	27.10	7.0	Grünthal and Wahlström, 2012	-	-
1343	10	18	40.90	28.00	7.1	Grünthal and Wahlström, 2012	-	-
1354	3	1	40.70	27.00	7.5	Grünthal and Wahlström, 2012	-	-
1419	-	-	41.00	34.0	7.5	Kondorskaya and Ulomov, 1999	-	-
1490	1	6	40.73	29.98	7.4	Yaltırak, 2015	110	Yaltırak, 2015
1509	10	14	40.70	28.80	7.5	Bulut et al., 2019	95	Yaltırak, 2015
1556	5	10	40.86	28.41	7.3	Yaltırak, 2015	65	Yaltırak, 2015
1569	12	13	40.82	27.83	7.3	Yaltırak, 2015	60	Yaltırak, 2015
1659	2	17	40.50	26.40	7.3	Grünthal and Wahlström, 2012	55	Yaltırak, 2015
1666	11	24	39.74	39.50	7.5	Ambraseys and Jackson, 1998	80	Barka, 1996
1668	8	17	41.00	36.00	8.1	Grünthal and Wahlström, 2012	480	Barka, 1996
1719	5	25	40.68	30.13	7.4	Bulut et al., 2019	110	Yaltırak, 2015
1766	5	22	40.92	28.58	7.3	Bulut et al., 2019	65	Yaltırak, 2015
1766	8	5	40.75	27.75	7.4	Bulut et al., 2019	60	Yaltırak, 2015
1912	8	9	40.65	27.20	7.4	Bulut et al., 2019	55	Gutzwiller, 1921
1939	12	26	39.80	39.51	7.9	Barka, 1996	360	Barka, 1996
1942	12	20	40.87	36.47	7.1	Ambraseys and Jackson, 1998	50	Barka, 1996
1943	11	26	41.05	33.72	7.6	Barka, 1996	260	Barka, 1996
1944	2	1	40.90	32.60	7.4	Barka, 1996	180	Barka, 1996
1957	5	26	40.60	31.00	7.0	Ambraseys and Jackson, 1998	40	Barka, 1996
1967	7	22	40.70	30.70	7.0	Barka, 1996	80	Barka, 1996
1999	8	17	40.70	30.00	7.4	Barka, 1996	145	Barka et al., 2002
1999	11	12	40.80	31.20	7.1	Grünthal and Wahlström, 2012	40	Akyüz et al., 2002

In this context, each fault section was analysed independently. The fault section-based slip deficits were calculated using the total duration since the latest large earthquake failing the section and the slip rate along the NAF (Reilinger et al., 2006). Table 2 presents the current fault section-based maximum slip deficits and corresponding moment magnitude potentials.

3. East-to-west deceleration of migrating earthquakes

Historical earthquake records have indicated that the NAF failure occurs with a systematic east-to-west migration of large earthquakes (Toksöz et al., 1979; Stein et al., 1997; Barka et al., 2002). By integrating all of the available historical data, it was identified that this spatiotemporal pattern was also relevant for the last 2 complete, in addition to the current incomplete, failures. Progress of the epicenters versus time were analysed to investigate the western tip of the cumulative failure in time (Figure 3).

Evolution of the NAF began in eastern Anatolia near Karlıova 13 to 11 Ma years ago (Şengör et al., 2005). Cumulative displacements along the NAF have suggested that the fault zone development progressively continued westward through Erzincan (cumulative displacement range from 50 to 70 km), Amasya (cumulative displacement range from 50 to 75 km), Çorum-Kargı (cumulative displacement range from 40 to 80 km), Bolu (cumulative displacement of 50 km), Sakarya-Pamukova (cumulative displacement range from 22 to 26 km), and finally arrived in the Marmara region (cumulative displacement range from 0.2 to 4.0 km) (Şengör et al., 1985; Barka and Gülen, 1988; Koçyiğit et al., 1988; Gaudemer, 1989; Sarıbudak et al., 1990; Bozkurt et al., 1997; Le Pichon et al., 2001;

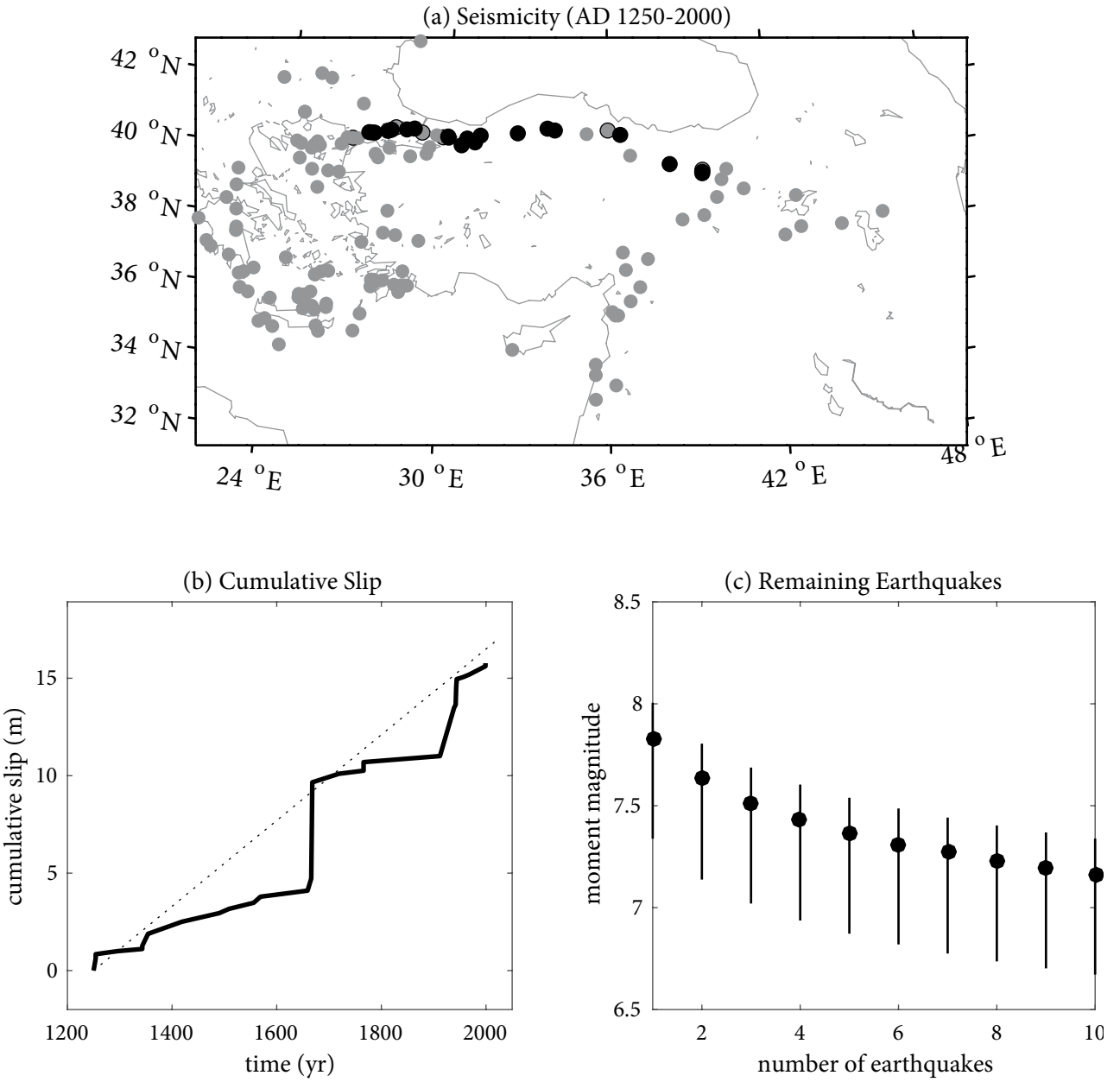

Figure 2. Historical earthquakes and corresponding cumulative slips along the NAF. a) Map view of historical earthquakes. Gray dots show the entire dataset and black dots show the analysed M ≥7.0 earthquakes along the NAF. b) Black line shows corresponding cumulative slips of the NAF that occurred with large earthquakes. Straight dashed line shows geodetic estimate of cumulative slip. c) The number of remaining large earthquakes required to complete the current failure. Circles show the number of earthquakes for corresponding magnitudes to complete the current failure of the NAF, and vertical bars show corresponding magnitude ranges in the case of variation in the locking depth range.

Hulbert-Ferrari, 2002; Herece and Akay, 2003; Şengör et al., 2005). It split into 2 strands in the west Bolu region of Turkey. The northern strand, which is located beneath the Sea of Marmara, currently hosts the highest tectonic slip rate when compared to the middle and southern strands (Reilinger et al., 2006). It is characterised by strong structural variations in the Marmara region, e.g., step overs, transpressional ridges, and transtensional basins,

Table 2. Current earthquake potential of the NAF.

Previous earthquake					Current potential	
Date	Latitude (°)	Longitude (°)	M	Length (km)	Maximum slip (m)	Maximum Mw
1912	40.65	27.20	7.4	65	2.70	7.1
1766	40.92	28.58	7.3	70	6.35	7.4
1766	40.75	27.75	7.4	80	6.35	7.5
1999	40.70	30.00	7.4	120	0.52	6.8
1967	40.70	30.70	7.0	85	1.32	6.9
1957	40.60	31.00	7.0	45	1.57	6.8
1944	40.90	32.60	7.4	150	1.90	7.2
1943	41.05	33.72	7.6	320	1.92	7.5
1942	40.87	36.47	7.1	40	1.95	6.9
1939	39.80	39.51	7.9	325	2.02	7.5

and substantial deviations of the fault strikes (Armijo et al., 1999; Yaltırak et al., 2002), when compared to the longer central and eastern segments (Barka, 1996).

East-to-west failure of the NAF also started near Karlıova, at ~40.0°E. It ruptured towards Bolu, near ~32.0°E, very fast. In previous complete failures, this nearly ~640-km section of the NAF failed during the 1666 Erzincan (M 7.5) and 1668 Kelkit Valley (M 8.1) earthquakes (Figure 3a). During the current incomplete failure, this section failed over a period of 5 years during the 1939 Erzincan (M 7.9), 1942 Niksar (M 7.1), 1943 Tosya (M 7.6), and 1944 Gerede (M 7.4) earthquakes (Figure 3a). In the western part of this region, however, the failure slowed down gradually, e.g., the remaining ~560-km-section of the NAF from Bolu in the east to Saros Bay in the west (27.0°E–32.0°E) failed over a period of 193 years, between the 1719 and 1912 earthquakes (Figure 3a).

The same deceleration is also presently taking place during the current incomplete failure, although failure has not yet entirely completed along the NAF (Figure 3a). In the western part of Bolu, a ~200-km section of the NAF has yet to rupture, despite the occurrence of the 1957 Abant (M 7.0), 1967 Mudurnu (M 7.0), 1999 İzmit (M 7.4), and 1999 Düzce (M 7.1) earthquakes. Epicenters have represented a parabolic function versus time during the previous 2 complete failures (Figure 3a). This function was compatible with the current incomplete failure and verified the deceleration of the east-to-west failure (Figure 3b). Complete failure of the NAF will last for 243 ± 3 years, based on the superimposed seismicity data from the historical earthquake catalogue compiled herein (Figures 3b and 4). This suggests that current failure, which began in 1939, might continue for 2182 ± 3 years.

4. Discussion

The slip deficit calculations herein were sensitive to the assumed fault area, and therefore, to the length and depth of the fault zone. The length of the fault zone has been well defined by the topography and bathymetry (Ketin, 1948; Şengör, 1979; Barka, 1992; Bulut et al., 2018). However, the coupled depth range of the fault zone varies between ~9 and ~11 km, based on previous seismicity studies (Aktar et al., 2004; Bulut et al., 2007; Bulut et al., 2018; Bulut et al., 2019). The slip deficit and potential magnitudes of the remaining NAF earthquakes within this depth range were analysed, and the results showed that the average slip deficit is presently 1.3 m along the NAF, suggesting that the NAF has the potential to generate up to 10 M ≥7.0 earthquakes to complete its current failure (Figure 2c). This will probably occur in the Sea of Marmara section, which has not reruptured since 1766. Historical catalog documents have shown that the Sea of Marmara segments of the NAF failed to generate M 7.3 or 7.4 earthquakes (Table 1). In this magnitude range, the calculations conducted in the current study have indicated that the NAF has the potential to generate a total of 4 to 6 earthquakes (Figure 2c). This was well in agreement with the number of historical earthquakes failing the Sea of Marmara earthquakes in each cycle, e.g., the 1490, 1509, 1556, 1569, and 1659 events in the first complete cycle, and the 1719, 1766a, 1766b, and 1912 events in the second complete cycle (Table 1). In this context, the NAF might generate a few more earthquakes in the Sea of Marmara region to complete its current failure. Alternatively, the same energy might be released by a single M 7.8 earthquake. This alternative scenario seems less likely based on the segmentation of the NAF and historical earthquake records along the currently unruptured section of the NAF.

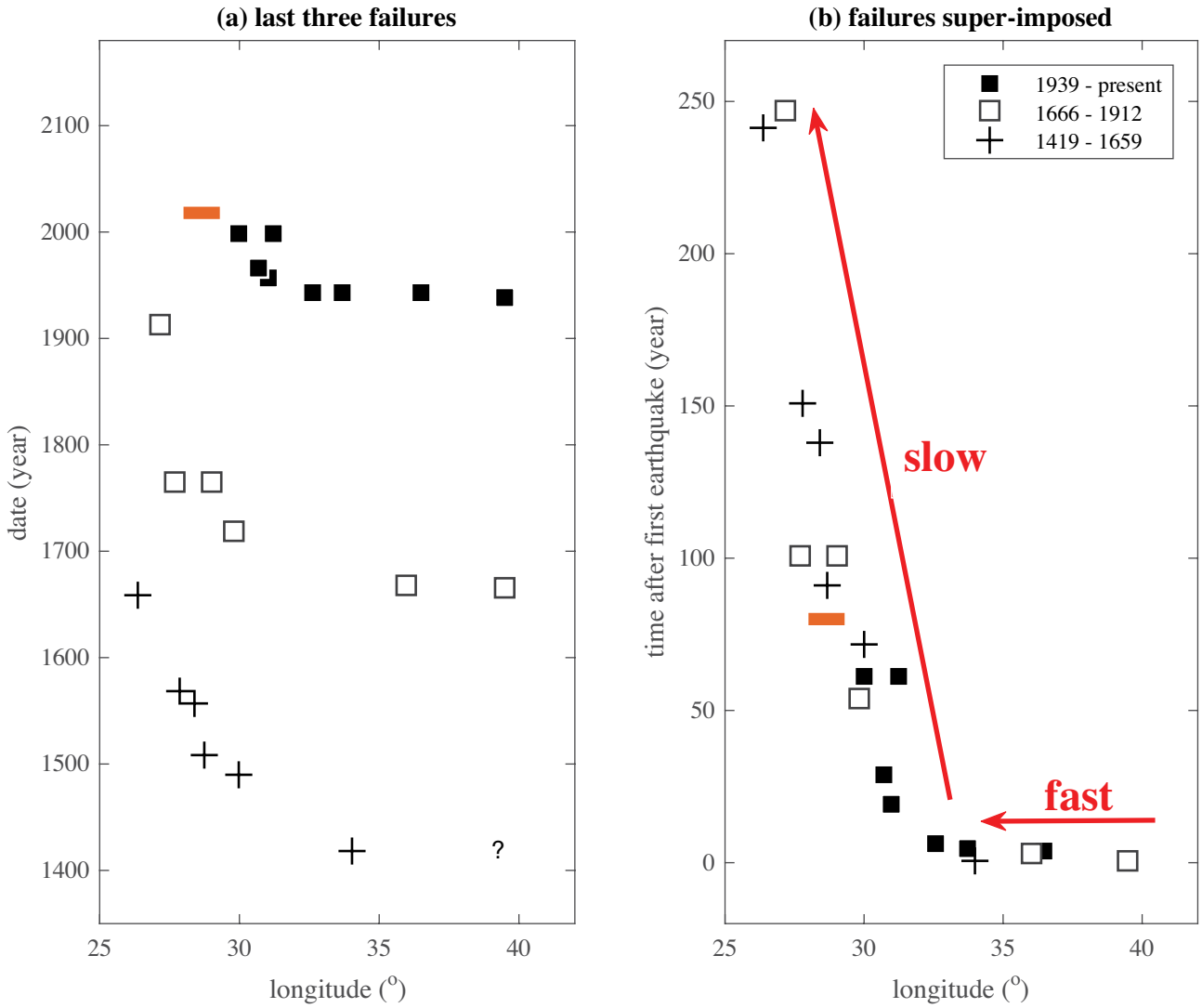

Figure 3. Stochastic behaviors of large earthquake epicenters along the NAF during the last 3 failures. Failures are shown by different symbols, as explained in the legend (plus: 1419–1659, open square: 1666–1912, solid square: 1939–present). The thick orange line indicates the current Marmara Seismic Gap: a) along-fault locations of large earthquakes versus the date, and b) along-fault locations of large earthquakes versus normalised time with respect to the first large earthquake of corresponding failure.

4.1. Unruptured Marmara section of the North Anatolian Fault

The segmentation of the NAF in the Marmara region is still under debate. The basic contradiction is as follows: 1) Single-segmented models have suggested that the entire Sea of Marmara section will be ruptured with a single large earthquake (Imren et al., 2001; Le Pichon et al., 2003; Şengor et al., 2014), 2) Multisegmented models, however, have suggested that the Sea of Marmara section will be ruptured as a series of relatively smaller size large earthquakes (Pull-apart-based models by Barka and Kadinsky-Cade, 1988; Barka, 1992; Ergun and Ozel, 1995; Wong et al., 1995; Parke et al., 1999; Okay et al., 2000; Siyako et al., 2000; Armijo et al., 2002), 3) Horsetail-type multisegmented model by Yaltırak (2002) and Yaltırak (2015) also suggests multi-segmentation of the NAF in the Sea of Marmara.

Based on the calculations herein, the Marmara segments that have most recently ruptured, i.e. in May 1766, August 1766, and August 1912, currently have the potential to generate Mw 7.5, Mw 7.4, and Mw 7.1 earthquakes, respectively (Table 2).

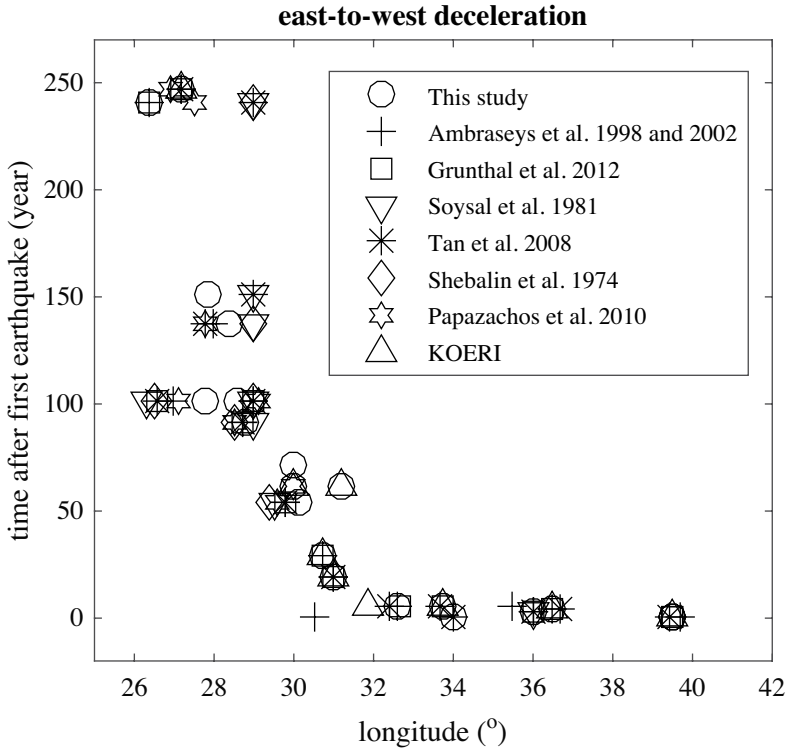

Figure 4. East-to-west deceleration of progressive failure of the NAF. Different historical earthquake catalogs were compared to verify the east-to-west decelerating migration of large earthquakes along the NAF.

How long does it take to fail the entire NAF? To address this question, we scanned through all available historical earthquake catalogues. There, Shebalin et al. (1974) and Soysal et al. (1981) did not report 19 and 13 earthquakes, respectively. Based on these incomplete catalogues, the duration of complete failure might change. Since both catalogues are significantly incomplete, they did not cover the entire fault zone and therefore, did not represent the entire failure. The historical catalogue compiled herein included 26 earthquakes that occurred between 1250 and 2000 AD. It indicated that complete failure of the NAF will last for 243 ± 3 years. However, paleoseismological studies, which have much larger error bounds in time, have reported longer recurrence intervals in different sections. Meghraoui et al. (2012) reported that the recurrence interval of large earthquakes over the last 1000 years was 323 ± 142 years along the Ganos (Mürefte) segment of the NAF. Drab et al. (2015) reported that the Çınarcık segment of the NAF reruptures every 256 to 321 years. These 2 studies focused on particular segments, while in the current study, the overall recurrence time for the entire NAF was observed. Moreover, their results included large error bounds of event times, while the historical earthquake catalog comprised absolute event times.

4.2. Role of strain partitioning on east-to-west decelerating failure

The western edge of the cumulative failure indicated the deceleration of the east-to-west migration of earthquakes along the NAF (Figures 3 and 4). In the short term, the section between the central and eastern (Çınarcık) segments of the Sea of Marmara section is more likely to fail, as this is the only dextral section of the NAF that has not failed since 1766. Overall, the east-to-west deceleration of migrating earthquakes has suggested that the remaining failure will take substantially longer than the failure of the fault that occurred with the1999 İzmit-Düzce earthquakes.

East-to-west deceleration of the failure can be alternatively explained by strain partitioning as the NAF splits into 3 basic strands in the eastern Marmara region. Previous GPS measurements have shown that the northern strand accommodates 85% of the total tectonic motion (Reilinger et al., 2006). To investigate, in detail, whether the southern strand accommodates comparably large slip rates or accumulates similar strain energies, the across-fault profiles of the GPS-derived horizontal velocity fields that were compiled by Bulut et al. (2019) were analysed (Figure 5). The profiles were defined in a N-S orientation,

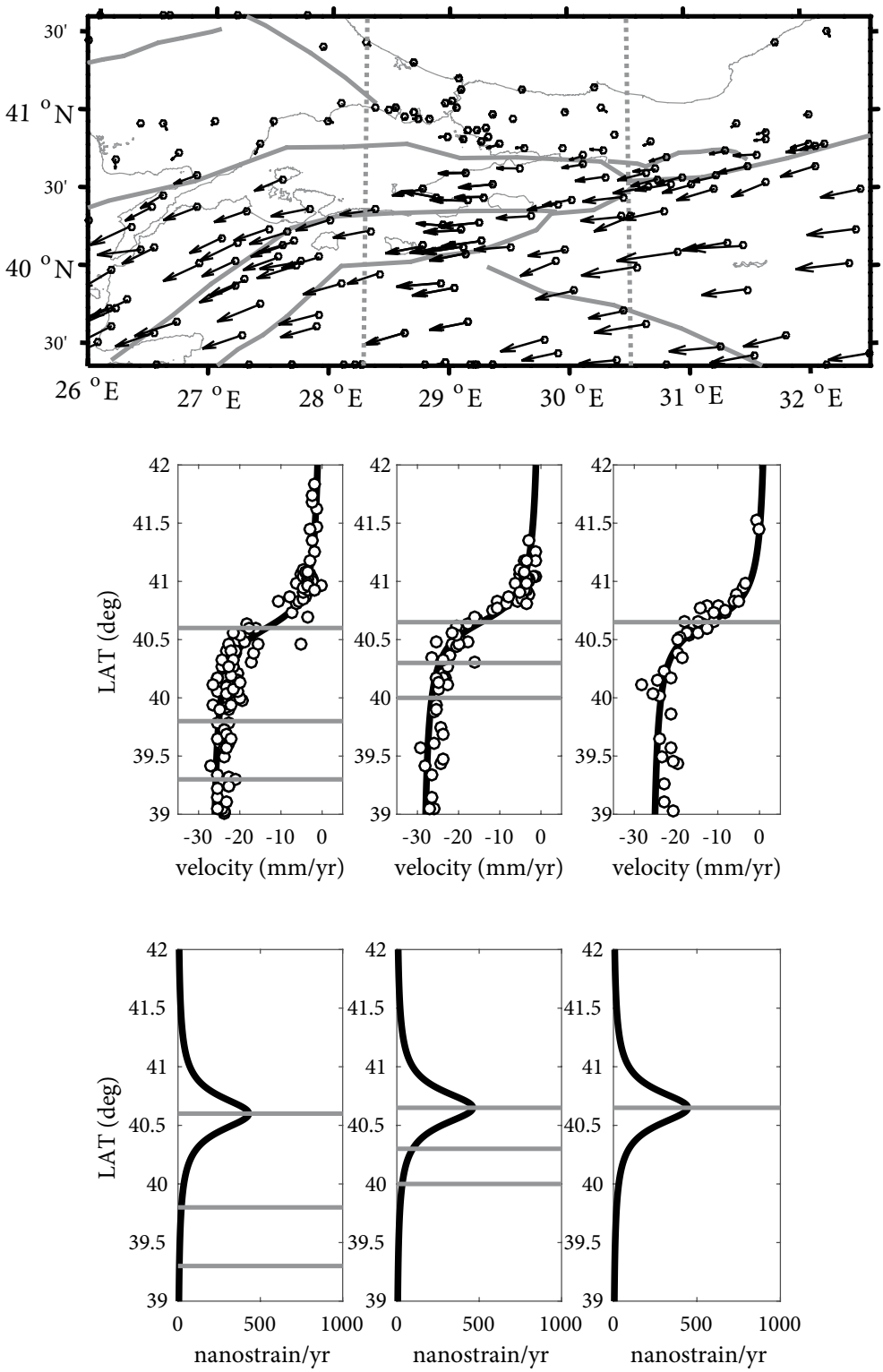

Figure 5. Eurasia-fixed GPS slip rates and corresponding strain profiles across the 3 strands of the NAF. GPS measurements were obtained from the work of Bulut et al., (2019). (Upper panel) Map view of the velocity field: Dark gray lines show major faults in the target area. Dashed gray lines show the profile boundaries. Arrows indicate the horizontal tectonic velocity field derived by GPS measurements. Middle and lower panels: Corresponding across-fault profiles of GPS velocity fields and strain rates. Gray lines indicate locations of subparallel strands of the NAF along slip and strain profiles in middle and lower panels.

across the strands of the NAF in the Marmara region. These 3 profiles verified that the majority of the slip rates, as well as the strain accumulation, is seen in the northern part of 40.40°N, where only the northern strand of the NAF operates (Figure 5, lower panels). This verified that most of the slip and therefore, the strain, is accommodated along the northern strand of the NA; hence, strain partitioning does not play a major role in the deceleration of the east-to-west progressive failure.

5. Conclusion

The following conclusions can be drawn from this research: 1) According to the current stage of slip deficit, the NAF has the potential to accommodate a few more M ≥7.0 earthquakes to complete its current failure, 2) Simultaneous failure of the remaining section as a single event would generate a M 7.8 earthquake. However, historical records have suggested that this will not occur as a single event, 3) M ≥7.0 earthquakes migrate to the west with an east-to-west decelerating pattern, The deceleration starts around the western tip of the 1944 Gerede rupture, 4) This suggests that the remaining failure will take substantially longer than the failure that occurred between the 1939 Erzincan (M 7.9) earthquake and the 1999 İzmit-Düzce (M 7.4 and M 7.1) earthquakes, 5) Complete failure of the NAF will last for 243 ± 3 years, 6) East-to-west deceleration of the failure cannot be verified by strain partitioning, as most of the tectonic deformation presently occurs on the northern strand of the NAF.

Acknowledgment

The study is supported by the research project "Slip deficit along Major Seismic Gaps in Turkey", which has been funded by the Boğaziçi University Fund of Scientific Research Projects (project number: 18T03SUP4). The authors thank the manuscript editor Serdar Akyüz, and the two anonymous referees for their constructive reviews. The authors also thank The Science Academy Turkey for supporting the study through the Young Scientist Award (BAGEP), which has been given to Fatih Bulut in 2020.

References

Aki K (1966). Generation and ropagation of G Waves from the Niigata Earthquake of June 16, 1964: Part 1. A statistical analysis, Bulletin of the Earthquake Research Institute, University of Tokyo 44.1 (1966): 23-72.

Aktar M, Dorbath C, Arpat E (2004). The seismic velocity and fault structure of the Erzincan basin, Turkey, using local earthquake tomography. Geophysical Journal International 156 (3): 497-505.

Akyuz HS, Hartleb R, Barka A, Altunel E, Sunal G et al. (2002). Surface rupture and slip distribution of the 12 November 1999 Düzce earthquake (M 7.1), North Anatolian fault, Bolu, Turkey. Bulletin of the Seismological Society of America 92 (1): 61-66.

Ambraseys NN, Jackson JA (1998). Faulting associated with historical and recent earthquakes in the Eastern Mediterranean region. Geophysical Journal International 133 (2): 390-406.

Armijo R, Meyer B, Hubert A, Barka A (1999). Westward propagation of the North Anatolian fault into the northern Aegean: timing and kinematics. Geology 27 (3): 267-270.

Armijo R, Meyer B, Navarro S, King G, Barka A (2002). Asymmetric slip partitioning in the Sea of Marmara pull-apart: a clue to propagation processes of the North Anatolian fault? Terra Nova 14 (2): 80-86.

Barka AA, Kadinsky-Cade K (1988). Strike-slip fault geometry in Turkey and its influence on earthquake activity. Tectonics 7 (3): 663-684.

Barka A (1996). Slip distribution along the North Anatolian fault associated with the large earthquakes of the period 1939 to 1967. Bulletin of the Seismological Society of America 86 (5): 1238-1254.

Barka A, Gülen L (1988). New constraints on age and total offset of the North Anatolian Fault Zone: implications for tectonics of the eastern Mediterranean region. METU Journal of Pure and Applied Sciences 31: 39-63.

Barka AA (1992). The North Anatolian Fault Zone. Annales Tectonicae 6: 164-195.

Barka A, Akyuz HS, Altunel E, Sunal G, Cakir Z et al. (2002). The surface rupture and slip distribution of the 17 August 1999 Izmit earthquake (M 7.4), North Anatolian Fault. Bulletin of the Seismological Society of America 92 (1): 43-60.

Bozkurt E, Holdsworth BK, Koçyigit A (1997). Implications of Jurassic chert identified in the Tokat Complex, northern Turkey. Geological Magazine 134 (1): 91-97.

Bulut F, Bohnhoff M, Aktar M, Dresen G (2007). Characterization of aftershock-fault plane orientations of the 1999 İzmit (Turkey) earthquake using high-resolution after shock locations. Geophysical Research Letters 34 (20). doi: 10.1029/2007GL031154

Bulut F, Bohnhoff M, Eken T, Janssen C, Kılıç T et al. (2012). The East Anatolian Fault Zone: seismotectonic setting and spatiotemporal characteristics of seismicity based on precise earthquake locations. Journal of Geophysical Research: Solid Earth 117 (B7).

Bulut F, Özener H, Doğru A, Aktuğ B, Yaltırak C (2018). Structural setting along the Western North Anatolian Fault and its influence on the 2014 North Aegean Earthquake (Mw 6.9). Tectonophysics 745: 382-394.

Bulut F, Aktuğ B, Yaltırak C, Doğru A, Özener H (2019). Magnitudes of future large earthquakes near İstanbul quantified from 1500 years of historical earthquakes, present-day microseismicity and GPS slip rates. Tectonophysics 764: 77-87.

Drab L, Hubert-Ferrari A, Schmidt S, Martez P, Carlut J et al. (2015). Submarine earthquake history of the Çınarcık segment of the North Anatolian Fault in the Marmara Sea, Turkey. Bulletin of the Seismological Society of America 105 (2A): 622-645.

Ergün M, Özel E (1995). Structural relationship between the Sea of Marmara basin and the North Anatolian Fault Zone. Terra Nova 7 (2): 278-288.

Gaudemer Y (1989). River offsets across active strike-slip faults. Annales Tectonicoe 3: 55-76.

Grünthal G, Wahlström R (2012). The European-Mediterranean earthquake catalogue (EMEC) for the last millennium. Journal of Seismology 16 (3): 535-570.

Gutzwiller OW (1921). Beitrage zur Geologie der Umgebung von Merfete am Marmara-Meere. PhD Thesis, Universitat Basel. (in German).

Herece E, Akay E (2003). Atlas of North Anatolian Fault (NAF). Ankara, Turkey: General Directorate of Mineral Research and Exploration, Special Publication series-2, 61: 13.

Imren C, Le Pichon X, Rangin C, Demirbağ E, Ecevitoğlu B et al. (2001). The North Anatolian Fault within the Sea of Marmara: a new interpretation based on multi-channel seismic and multi-beam bathymetry data. Earth and Planetary Science Letters 186 (2): 143-158.

Jackson DD (2003). Earthquake Prediction and Forecasting. In: Jackson DD. (editor), AGU Geophysical Monograph Series, "State of the Planet",. Washington, D.C., USA: American Geophysical Union, pp. 335-348.

Kanamori H (1983). Magnitude scale and quantification of earthquakes. Tectonophysics 93 (3-4): 185-199.

Ketin I (1948). Über die tektonisch-mechanischen Folgerungen aus den grossen anatolischen Erdbeben des letzten Dezenniums. Geologische Rundschau 36 (1): 77-83 (in German).

Koçyiğit A, Özkan S, Rojay B (1988). Examples from the forearc basin remnants at the active margin of northern Neo-Tethys; development and emplacement ages of the Anatolian Nappe, Turkey. METU Journal of Pure and Applied Sciences 21 (1-3): 183-210.

Kondorskaya NV, Ulomov VI (1999). Special catalogue of earthquakes of the Northern Eurasia (SECNE). URL: http:// www. seismo. ethz. ch/gshap/neurasia/nordasiacat.txt.

Le Pichon X, Şengör AMC., Demirbağ E, Rangin C, Imren, C., et al. (2001). The active main Marmara fault. Earth and Planetary Science Letters 192 (4): 595-616.

Le Pichon X, Chamot-Rooke N, Rangin C, Sengör AMC (2003). The North Anatolian fault in the sea of marmara. Journal of Geophysical Research: Solid Earth 108 (B4).

Meghraoui M, Aksoy ME, Akyüz HS, Ferry M, Dikbaş A, et al. (2012). Paleoseismology of the North Anatolian fault at Güzelköy (Ganos segment, Turkey): size and recurrence time of earthquake ruptures west of the Sea of Marmara. Geochemistry, Geophysics, Geosystems 13 (4).

Okay AI, Kaşlılar-Özcan A, Imren C, Boztepe-Güney A, Demirbağ E et al. (2000). Active faults and evolving strike-slip basins in the Marmara Sea, northwest Turkey: a multichannel seismic reflection study. Tectonophysics 321 (2): 189-218.

Parke JR, Minshull TA, Anderson G, White RS, McKenzie D et al. (1999). Active faults in the Sea of Marmara, Western Turkey, imaged by seismic reflection pro¢ les. Terra Nova 11: 223-227.

Reilinger R, McClusky S, Vernant P, Lawrence S, Ergintav S et al. (2006). GPS constraints on continental deformation in the Africa-Arabia-Eurasia continental collision zone and implications for the dynamics of plate interactions. Journal of Geophysical Research: Solid Earth 111 (B5).

Papazachos BC, Comninakis PE, Karakaisis GF, Karakostas BG, Papaioannou CA et al. (2000). A catalogue of earthquakes in Greece and surrounding area for the period 550BC-1999. Publication of the Geophysical Laboratory, University of Thessaloniki 1: 333.

Sarıbudak M, Sanver M, Sengör AMC, Görür N (1990). Palaeomagnetic evidence for substantial rotation of the Almacik Flake within the North Anatolian fault zone, NW Turkey. Geophysical Journal International 102 (3): 563-568.

Sengör AMC (1979). The North Anatolian transform fault: its age, offset and tectonic significance. Journal of the Geological Society 136 (3): 269-282.

Şengör AMC, Görür N, Şaroğlu F (1985). Strike-slip faulting and related basin formation in zones of tectonic escape: Turkey as a case study. In: BIDDLE, K. & CHRISTIE-BLICK, N. (eds), Strike-Slip Deformation, Basin Formation and Sedimentation. Society of Economic Paleontologists and Mineralogists, Special Publications 37, 227–264.

Şengör AMC, Tüysüz O, Imren C, Sakınç M, Eyidoğan H et al. (2005). The North Anatolian fault: a new look. Annual Review of Earth and Planetary Sciences 33: 37-112.

Şengör AMC, Grall C, İmren C, Le Pichon X, Görür N et al. (2014). The geometry of the North Anatolian transform fault in the Sea of Marmara and its temporal evolution: implications for the development of intracontinental transform faults. Canadian Journal of Earth Sciences 51 (3): 222-242.

Shebalin NV, Karnik V, Hadzievski D (1974). Catalogue of earthquakes of the Balkan region, I, UNDP-UNESCO Survey of the seismicity of the Balkan region.

Siyako M, Tanıs T, Saroglu F (2000). Marmara Denizi'nin aktif fay geometrisi (Active fault geometry of the Marmara Sea). Bilim ve Teknik 388: 66-71. (in Turkish)

Stein RS, Barka AA, Dieterich JH (1997). Progressive failure on the North Anatolian fault since 1939 by earthquake stress triggering. Geophysical Journal International 128 (3): 594-604.

Soysal H, Sipahioğlu S, Kolçak D, Altınok Y (1981). Türkiye ve çevresinin tarihsel deprem kataloğu. TÜBİTAK Project Report, no: TBAG341 (in Turkish).

Tan O, Tapirdamaz MC, Yörük A (2008). The earthquake catalogues for Turkey. Turkish Journal of Earth Sciences 17 (2): 405-418.

Taymaz T, Jackson J, McKenzie D (1991). Active tectonics of the north and central Aegean Sea. Geophysical Journal International 106 (2): 433-490.

Toksöz MN, Shakal AF, Michael AJ (1979). Space-time migration of earthquakes along the North Anatolian fault zone and seismic gaps. Pure and Applied Geophysics 117 (6): 1258-1270.

Wong HK, Lüdmann T, Ulug A, Görür N (1995). The Sea of Marmara: a plate boundary sea in an escape tectonic regime. Tectonophysics 244 (4): 231-250.

Yaltırak C (2002). Tectonic evolution of the Marmara Sea and its surroundings. Marine Geology 190 (1): 493-529.

Yaltırak C (2015). Marmara Denizi ve çevresinde tarihsel depremlerin yerleri ve anlamı. İTÜ Vakfı Dergisi 67: 51-58 (in Turkish).

Yaltırak C, İşler EB, Aksu AE, Hiscott RN (2012). Evolution of the Bababurnu Basin and shelf of the Biga Peninsula: western extension of the middle strand of the North Anatolian Fault Zone, Northeast Aegean Sea, Turkey. Journal of Asian Earth Sciences 57: 103-119.

Yaltırak C, Şahin M (2017). 10th of July, 1894 Istanbul Earthquake (Marmara Sea, Turkey). In EGU General Assembly Conference Abstracts (p. 12465).